SUPPLEMENTAL INFORMATION

SUPPLEMENTAL FIGURES

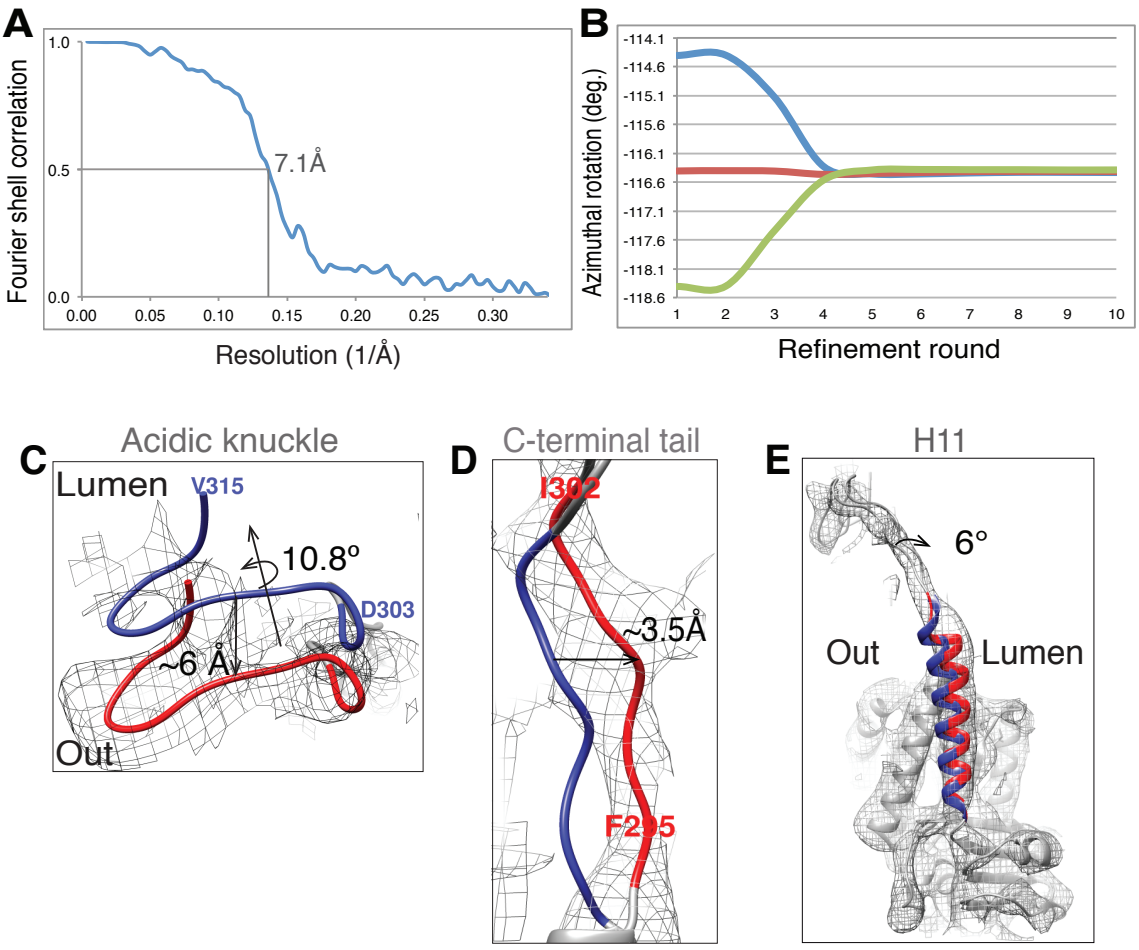

Figure S1, related to Figure 2. Resolution estimation and helical parameter validation test for the cryo-EM reconstruction. Flexible fitting of the atomic model into the cryo-EM map. (**A**) Resolution estimate for the cryo-EM reconstruction of the $PhuZ_{201}$ filament. FSC indicates the resolution of the reconstruction is 7.1 Å by the FSC 0.5 criterion and likely better as "gold standard" refinement was performed. (**B**) Convergence of azimuthal rotation per subunit from different starting symmetries. Three independent reconstructions were performed starting from different values (-118.4º, -116.4º or -114.4º) for the azimuthal rotation angle per subunit. In the forth round of refinement the value for the angle converged to -116.4°, indicating a stable and consistent solution for the helical symmetry. (**C**)-(**E**) Atomic model is colored by the scheme: C-terminus (H11 and the C-terminal tail) is in blue and red; N-terminal and activation domains, and H7 are in gray. Cryo-EM map density is represented as a gray wire mesh. Out is the outer surface and Lumen is the inside of the filament. In blue is the conformation of the C-terminus as in the crystal packing (3r4v) (Kraemer et al., 2012) and in red is the conformation as in the three-stranded filament. Flexible fitting: (**C**) The C-terminal tail was rotated 10.8˚ counterclockwise together with the longitudinal subunit and translated by 3.5 Å towards the adjacent strand (**D**); (**E**) H11 was tilted 6˚ towards the lumen.

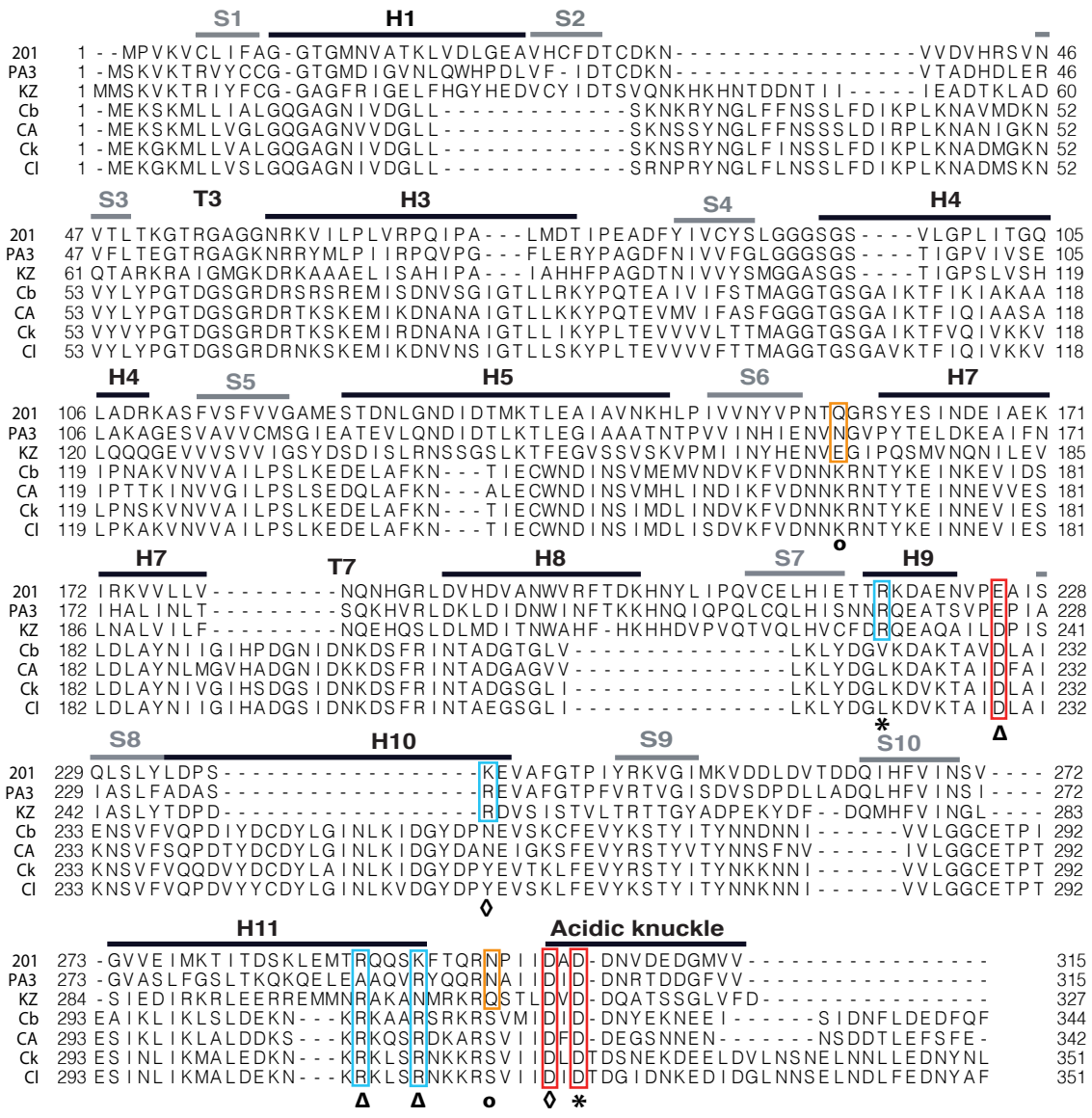

Figure S2, related to Figure 3. Conservation of residues predicted to form lateral contacts among the PhuZ family and *Clostridial* chromosomal tubulin homologues. Alignment of amino acid sequences was performed using Mafft with default settings in Jalview (Waterhouse et al., 2009). The amino acid positions are indicated at the beginning and at the end of each line. Secondary structural elements of $PhuZ_{201}$ are abbreviated as: α-helices (**H**), β-strands (**S**) and loops/turns (**T**). Conserved residues, predicted to form the lateral interface, are highlighted: negatively charged (red), positively charged (blue), and polar (orange). D303 contacts K238 (♢), D305 contacts R217 (∗), N299 contacts Q157 (**O**); R290 or R294 ($PhuZ_{PA3}$) contacts E225 (**Δ**). Abbreviations for sequences encoding tubulin homologues: 201 (phage 201Φ2-1); PA3 (phage ΦPA3); KZ (phage ΦKZ); Cb (*C. butyricum* 5521); CA (*C. acetobutylicum* ATCC824); Ck (*C. kluyveri* DSM555) and Cl (*C.cellulovorans* 743B).

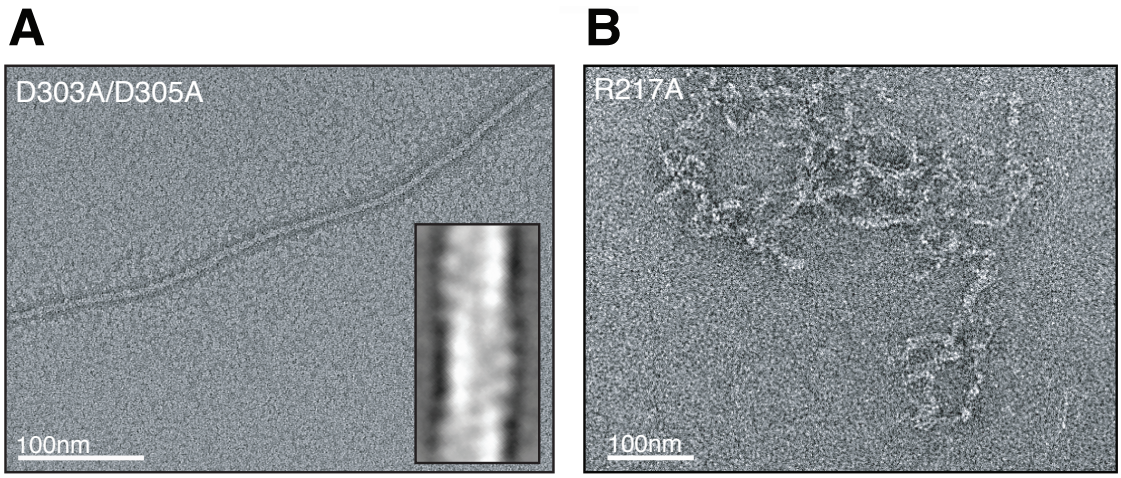

Figure S3, related to Figure 4. Mutations to residues predicted to mediate lateral contacts disrupt $PhuZ_{201}$ assembly *in vitro*. Sections of micrographs of negatively stained $PhuZ_{201}$ double mutant (D303A/D305A) (**A**) and single mutant (R217A) (**B**). (**A**) D303A/D305A forms rare three-stranded filaments as indicated by the reference-free 2D average in the inset. (**B**) R217A forms amorphous structures in a nucleotide-dependent manner.

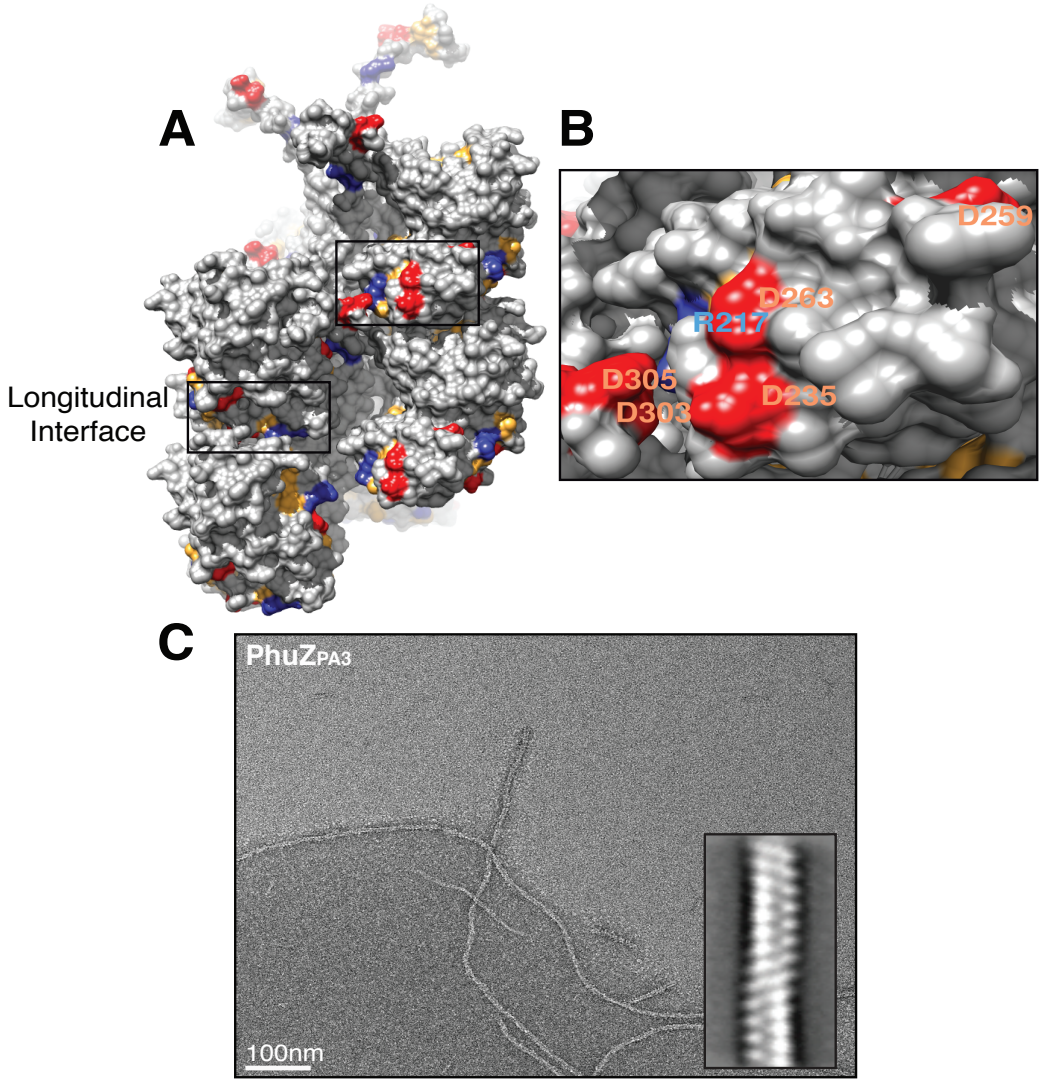

Figure S4. PhuZ family tubulins assemble three-stranded filaments. (**A**) and (**B**) In yellow (hydrophobic and polar), red (negatively charged) and blue (positively charged) surfaces having 100% amino acid sequence conservation among $PhuZ_{201,}$ $PhuZ_{PA3}$ and $PhuZ_{KZ}$. Non-conserved surfaces are in gray. Amino acid sequences of $PhuZ_{201,}$ $PhuZ_{PA3}$ and $PhuZ_{KZ}$ were aligned using Jalview Mafft option (Waterhouse et al., 2009) and molecular surfaces of the $PhuZ_{201}$ filament atomic model were "rendered by conservation" using UCSF Chimera (Pettersen et al., 2004). The conserved surfaces are outlined on the atomic structure (**A**) and some are magnified in the inset (**B**). In addition to the conservation of the longitudinal and lateral surfaces, there is a negatively charged surface formed by D235, D259 and D263 (**B**) that may mediate protein-protein interactions. (**C**) Section of a micrograph of negatively stained $PhuZ_{PA3}$ filaments polymerized in 1mM GMPCPP. Inset: reference free 2D average of 500 segments of $PhuZ_{PA3}$ polymer indicates that $PhuZ_{PA3}$ forms three-stranded filaments.

Mutations	Critical concentration ± error, (μM)
Wild type	2.5 ± 0.1
R217A	> 30
D303A	3.7 ± 0.2
D305A	4.1 ± 0.4
D303A/D305A	9.4 ± 0.3
R217D	> 30
D305R	8.0 ± 0.2
R217D/D305R	5.9 ± 0.3

Table S1, related to Figure 4. Critical concentrations of $PhuZ_{201}$ wild type and mutant constructs.

Movie S1, related to Figure 2. Pseudo-atomic model of $PhuZ_{201}$ filament. Gray wire mesh represents 3D cryo-EM density map fitted with the atomic model of $PhuZ_{201}$ in red. Flexible fitting was applied to the C-terminus before docking the atomic model into the map. The movie rotates the pseudo-atomic model around an axis parallel to the long axis of the $PhuZ_{201}$ filament.

Movie S2, related to Figure 6. PhuZ dimer rearranges upon incorporation into the filament lattice. Morph movie shows differences between packing of the $PhuZ_{201}$-GDP dimer (3r4v) (Kraemer et al., 2012) versus $PhuZ_{KZ}$-GDP (3ZBQ) (Aylett et al., 2013) and the three-stranded GMPCPP filament. To make the morph longitudinal dimers from the three structures were aligned using the N-terminal domains of the subunits at the minus ends of the dimers. Alpha carbons of the residues, predicted to mediate lateral contacts, are shown as spheres. In the presence of the γ-phosphate (GMPCPP filament) a tense inter-subunit interface is formed. Both inter-subunit twisting and C-terminal bending towards the laterally adjacent dimer are required to establish the lateral interface.

SUPPLEMENTAL EXPERIMENTAL PROCEDURES

Molecular Fitting. To optimize the fit of the $PhuZ_{201}$ atomic model (Kraemer et al., 2012) into the cryo-EM map, the atomic model was initially docked into the map using "Fit in Map" option in UCSF Chimera (Pettersen et al., 2004), and the fit of H11 and the C-terminal tail were further optimized using Coot (Emsley and Cowtan, 2004). Next, the helical parameters (-116.4° rotation and 14.4 Å axial rise per subunit) were applied to the atomic structure to obtain a pseudo-atomic model of the filament. The cross-correlation coefficients for the atomic model, before and after the application of the flexible fitting, with the segment of the cryo-EM reconstruction, corresponding to a single subunit, was measured using "Fit in Map" option in UCSF Chimera (Pettersen et al., 2004).

Structure Analysis and Comparison. Visualization and comparative analysis were performed using UCSF Chimera (Pettersen et al., 2004). Buried surface area values were measured using CCP4 "areaimol" (Lee and Richards, 1971) (E.B.Saff and A.B.J.Kuijlaars, *The Mathematical Intelligencer*, **19**, 5-11 (1997) http://www.math.vanderbilt.edu/~esaff/texts/161.pdf).

REFERENCES

Emsley, P., and Cowtan, K. (2004). Coot: model-building tools for molecular graphics. Acta crystallographica Section D, Biological crystallography *60*, 2126-2132.

Lee, B., and Richards, F.M. (1971). The interpretation of protein structures: estimation of static accessibility. Journal of molecular biology *55*, 379-400.

Waterhouse, A.M., Procter, J.B., Martin, D.M., Clamp, M., and Barton, G.J. (2009). Jalview Version 2--a multiple sequence alignment editor and analysis workbench. Bioinformatics *25*, 1189-1191.